ANL/CFCT-22/43

Property Measurements of the $NaCl$-$PuCl_3$ Molten Salt System

Chemical and Fuel Cycle Technologies Division

About Argonne National Laboratory
Argonne is a U.S. Department of Energy laboratory managed by UChicago Argonne, LLC under contract DE-AC02-06CH11357. The Laboratory's main facility is outside Chicago, at 9700 South Cass Avenue, Argonne, Illinois 60439. For information about Argonne and its pioneering science and technology programs, see www.anl.gov.

DOCUMENT AVAILABILITY

Online Access: U.S. Department of Energy (DOE) reports produced after 1991 and a growing number of pre-1991 documents are available free at OSTI.GOV (http://www.osti.gov/), a service of the US Dept. of Energy's Office of Scientific and Technical Information.

Reports not in digital format may be purchased by the public from the National Technical Information Service (NTIS):
U.S. Department of Commerce
National Technical Information Service
5301 Shawnee Rd
Alexandria, VA 22312
www.ntis.gov
Phone: (800) 553-NTIS (6847) or (703) 605-6000
Fax: (703) 605-6900
Email: **orders@ntis.gov**

Reports not in digital format are available to DOE and DOE contractors from the Office of Scientific and Technical Information (OSTI):
U.S. Department of Energy
Office of Scientific and Technical Information
P.O. Box 62
Oak Ridge, TN 37831-0062
www.osti.gov
Phone: (865) 576-8401
Fax: (865) 576-5728
Email: **reports@osti.gov**

Disclaimer
This report was prepared as an account of work sponsored by an agency of the United States Government. Neither the United States Government nor any agency thereof, nor UChicago Argonne, LLC, nor any of their employees or officers, makes any warranty, express or implied, or assumes any legal liability or responsibility for the accuracy, completeness, or usefulness of any information, apparatus, product, or process disclosed, or represents that its use would not infringe privately owned rights. Reference herein to any specific commercial product, process, or service by trade name, trademark, manufacturer, or otherwise, does not necessarily constitute or imply its endorsement, recommendation, or favoring by the United States Government or any agency thereof. The views and opinions of document authors expressed herein do not necessarily state or reflect those of the United States Government or any agency thereof, Argonne National Laboratory, or UChicago Argonne, LLC.

ANL/CFCT-22/43

Property Measurements of the NaCl-$PuCl_3$ Molten Salt System

---

prepared by
T. Lichtenstein, L. Gardner, and M.A. Rose
Chemical and Fuel Cycle Technologies Division, Argonne National Laboratory

October 31, 2022

CONTENTS

LIST OF TABLES

LIST OF FIGURES

1. Introduction

Thermochemical and thermophysical property values of several salt compositions of interest are needed by molten salt reactor (MSR) developers to design, license, and operate their reactors. Thermochemical and thermophysical properties being measured at Argonne include thermal transitions, phase behavior, and heat capacity, density, surface tension, volumetric thermal expansion of the liquid phase, thermal diffusivity, thermal conductivity, and viscosity.

Properties of salt compositions in the binary NaCl-$PuCl_3$ system that may be used as a fuel bearing salt are being measured. The eutectic composition of the NaCl-$PuCl_3$ system has been estimated to have between 36 and 38.3 mol % $PuCl_3$ (Yin et al., 2020, Beneš and Konings, 2008, and Bjorklund et al., 1959). A complete understanding of the salt behavior at compositions near the eutectic composition is essential to the design, licensing and operation of a NaCl-$PuCl_3$ fueled reactor. Compositions of NaCl-$PuCl_3$ salt mixtures with between 20 and 59.9 mol % $PuCl_3$ were synthesized and their thermal behavior was measured by using differential scanning calorimetry to understand the effect of off-eutectic compositions on the salt behavior. Heat capacity was measured for the solid phases of salt mixtures with 20, 37.4, 38.3 and 59.9 mol % $PuCl_3$ and the liquid phases of mixtures with 37.4 and 38.3 mol % $PuCl_3$. It was recently demonstrated that the value of the heat capacity has a large effect on predicted salt temperatures during molten salt reactor operation and that an accurate determination of this property value is required for reliable design (Rose and Creasman, 2022). The heat capacities of NaCl-$PuCl_3$ salts measured in this study will be made available to reactor developers by incorporating measured data into the Molten Salt Thermal Properties Database (MSTDB-TC, V2.0).

Property values at temperatures higher than can be achieved using currently available devices are needed to understand and model the behavior of the salts over the full range of transient and accident scenarios. In the case of differential scanning calorimetry measurements, the functional range of sealable gold cells is limited to approximately 800 °C due to the softening and distortion of cells at higher temperatures. The use of alternative materials to fabricate a robust sealable encapsulation device for use in differential scanning calorimetry (DSC) measurements at high temperatures is being evaluated at Argonne. Progress on the development of these cells to provide data at elevated temperatures is included in this report.

2. Synthesis

The series of NaCl-$PuCl_3$ salt mixtures was prepared by adding appropriate amounts of NaCl to $PuCl_3$ to achieve the targeted compositions. The $PuCl_3$ source material was synthesized from PuO_2 stock in two steps. First, PuO_2 was reduced to plutonium metal by reaction with stoichiometric quantities of metallic calcium in a boron nitride crucible. The PuO_2 and calcium reagents, which are shown in Figure 1a, were covered with an excess of $CaCl_2$ to provide flux, as shown in Figure 1b. The reagents were then heated to 780 °C in a furnace and allowed to react for 6 h while being mixed using a tungsten stir rod rotated at 300 rpm.

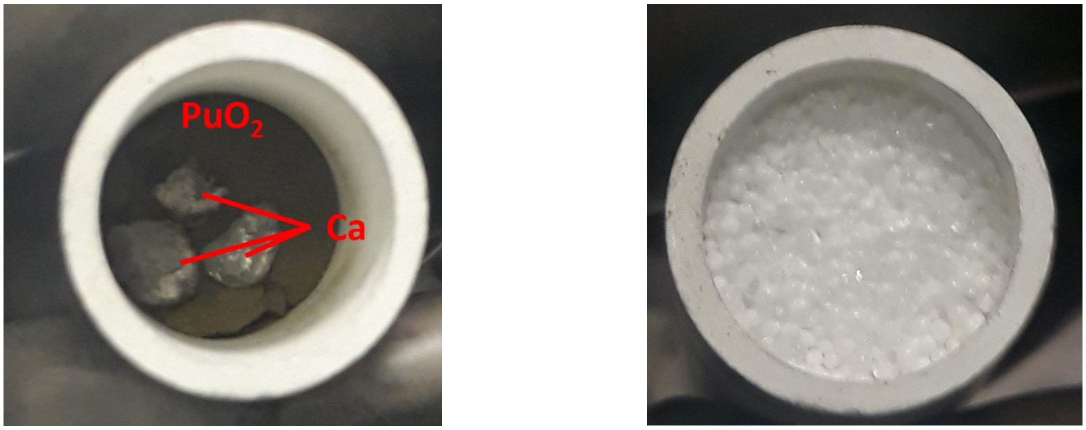

(a) (b)

Figure 1. Photographs of (a) the loaded PuO_2 and calcium in a boron nitride crucible and (b) the $CaCl_2$ flux covering the reagents.

The stir rod was raised out of the flux and the crucible was allowed to cool completely to solidify the products. The crucible was removed from the furnace and photographed. As shown in Figure 2a, the top of product was coated with a black material (which is plutonium metal) with no visible inclusions. The material in the middle third of the product, which is shown in Figure 2b after retrieval, was a mixture of black metallic plutonium (black), unreacted reagents, and CaO within a $CaCl_2$ matrix (green). The material in the bottom third of the product was a fused green material with no black inclusions that is shown in Figure 2c. This is expected to be a mixture of unreacted reagents and CaO in a $CaCl_2$ matrix. The metallic plutonium recovered from the top third of the crucible was chlorinated and the other materials were retained for future use.

(a) (b) (c)

Figure 2. Photographs of (a) the top portion of the metal reduction product in the crucible, which is plutonium metal, (b) recovered material from the middle portion of the product, and (c) the lower portion of material in the crucible.

The metallic plutonium was chlorinated by reaction with NH_4Cl in a 58-mL stainless steel vessel through the following reaction:

$$3NH_4Cl + Pu \rightarrow PuCl_3 + 6H_2 + 1.5\ N_2 \tag{1}$$

The plutonium metal was sealed in the vessel with excess NH_4Cl and the mixture heated to 350 °C and held overnight to form an intermediate compound. The container was opened and heated at 500 °C for 6 h to decompose the product. These chlorination steps were repeated to increase the degree of chlorination of the plutonium. A photograph of the final $PuCl_3$ product is provided in Figure 3. The product was dark green in color.

Figure 3. Photograph of the chlorinated plutonium product.

The $PuCl_3$ was transferred to a graphite crucible and dried NaCl was added to generate the series of salt compositions that were analyzed. The salt mixture with the lowest NaCl content was made first and increments of NaCl were added to generate the other salts. The salt compositions are listed in Table 1 based on the measured and calculated masses of $PuCl_3$ and NaCl in each mixture. The salt mixture made first is identified as Salt 1 in Table 1. The Salt 1 mixture was fused at 700 °C. The cooled salt was crushed and samples taken for use in thermal analysis and heat capacity measurements. The remaining mass of Salt 1 was measured and used to calculate the masses of $PuCl_3$ and NaCl and the appropriate mass NaCl to be added to generate Salt 2. The Salt 2 mixture was heated at 700 °C to fuse the salt, then crushed and sampled. This process was repeated by adding small amounts of NaCl to the remaining mass to generate the next target composition. Table 1 lists the masses of NaCl and $PuCl_3$ in each of the mixtures and the calculated compositions. Each of the seven compositions was crushed and sampled in the same manner.

Table 1. Batched Compositions of NaCl-$PuCl_3$ Salts

Salt ID	Batched Composition					
	Reagent mass[a], g		wt %		mol %	
	$PuCl_3$	NaCl	$PuCl_3$	NaCl	$PuCl_3$	NaCl
Salt 1	1.57096	0.17575	89.9	10.1	59.9	40.1
Salt 2	1.54439	0.26177	85.5	14.5	49.6	50.4
Salt 3	1.49099	0.40069	78.8	21.2	38.3	61.7
Salt 4	1.45638	0.40665	78.2	21.8	37.4	62.6
Salt 5	1.43919	0.42630	77.1	22.8	36.0	64.0
Salt 6	1.42213	0.55375	72.0	28.0	30.0	70.0
Salt 7	1.40393	0.93915	59.9	40.1	20.0	80.0

[a] Sum of calculated residual and added masses.

3. Thermal Analysis

Differential scanning calorimetry was used to measure the melting point of each NaCl-$PuCl_3$ mixture. Hermetically sealed gold sample crucibles (TA Instruments, Wood Dale, IL) were used to contain salts for analysis. The gold cells were cleaned before use by washing with water, degreasing with ethanol, and then washing again with water. The cells were allowed to air dry before being placed into an argon atmosphere glovebox that was maintained with less than 10 ppm oxygen. The empty gold cells were carefully weighed then loaded with crushed salt and sealed by using a mechanical sealer.

Thermal properties of the salt samples were measured by using a Netzsch (Model STA Jupiter 449C) standard thermal analyzer (STA) operated inside of an argon atmosphere glovebox. A continuous high purity argon purge inside of the instrument was used to maintain the atmosphere surrounding the sample at even lower oxygen and moisture conditions than the surrounding glovebox atmosphere during the measurements. The temperature measurement provided by the DSC instrument was calibrated before analyzing the salts by measuring the melting behaviors of five pure metal standards (tin, zinc, aluminum, silver, and gold) that have known melting points spanning the range from 231.9 to 1064.2 °C. Known masses of each standard were contained in open alumina crucibles. The measured onset temperatures are used by the DSC software to calibrate the instrument temperature response. The DSC response is affected by the placement of the cells in the instrument and by minor variances in the glovebox atmosphere during the analyses. Measured temperatures are typically accurate to within 2 °C of the melting points of the reference metals. This represents the accuracy of the measured melting temperatures of the salts.

Samples of the seven prepared salt compositions (Table 1) were analyzed to measure the melting temperatures and detect any additional phase transitions. Each sample heated in the STA to 650 °C at a heating rate of 20 °C min^{-1} to ensure the salt was well mixed before the analyses. The sample was allowed to cool to 300 °C and subsequently reheated at 5 °C min^{-1} from 300 to 650 °C to measure the melting point. Salt 7 (with 20 mol % $PuCl_3$) was heated to a maximum temperature of 700 °C because it was expected to have a higher melting temperature. The sample was allowed to cool and the heating scan was repeated. The repeatability of measurements made with the seven salts are shown in Figure 4. The repeatability of the duplicate measurements was used to confirm system stability. Minor effects of fluctuations in the glovebox pressure that occurred during the analyses are observed at temperatures higher than the melting peaks.

Figure 5 shows a comparison of representative DSC responses for the seven salt mixtures with the transitions marked. The transition temperatures occurring in each scan were determined by using either the onset, peak, or endpoint function in the Netzsch software PROTEUS® and the values are summarized in Table 2. Three reaction peaks were detected in analyses of Salts 1-4 that were made with the highest $PuCl_3$ contents: one with an onset temperature near 332 °C, one with a peak temperature near 363 °C, and a eutectic peak with an onset temperature near 457 °C. A shoulder indicating off-eutectic behavior was also evident in scans with these salts. The peak temperature is identified for reactions two and three because the onset temperatures for those reactions could not be identified by the software. Analyses of Salts 5-7 that were made with the lowest $PuCl_3$ contents showed three peaks: one with a peak temperature near 376 °C, one with an onset temperature near 439 °C, and a eutectic peak with an onset temperature near 457 °C. Each scan had a shoulder indicating off-eutectic behavior. The completion temperatures of the shoulders indicate complete melting (i.e., the liquidus temperature) and values are listed in Table 2. The peak temperatures for the eutectic reactions of the $PuCl_3$-rich compositions of Salts 1-4 are slightly lower than those for the $PuCl_3$-poor compositions of Salts 5-7 (476 ± 1 °C compared to 480.0 ± 2 °C). These peak temperatures are listed in Table 2.

Simple eutectic behavior is not observed in the results for any of the seven salts. The averages of transition temperatures determined for the seven salts are provided to show the similarity of values for different compositions is within or near the measurement uncertainty of approximately 2 °C. These analyses indicate the Salt 4 mixture is closest to the pure eutectic composition. Compositional determination by wet chemical methods will be performed to verify the composition of Salt 4 and the other salt mixtures.

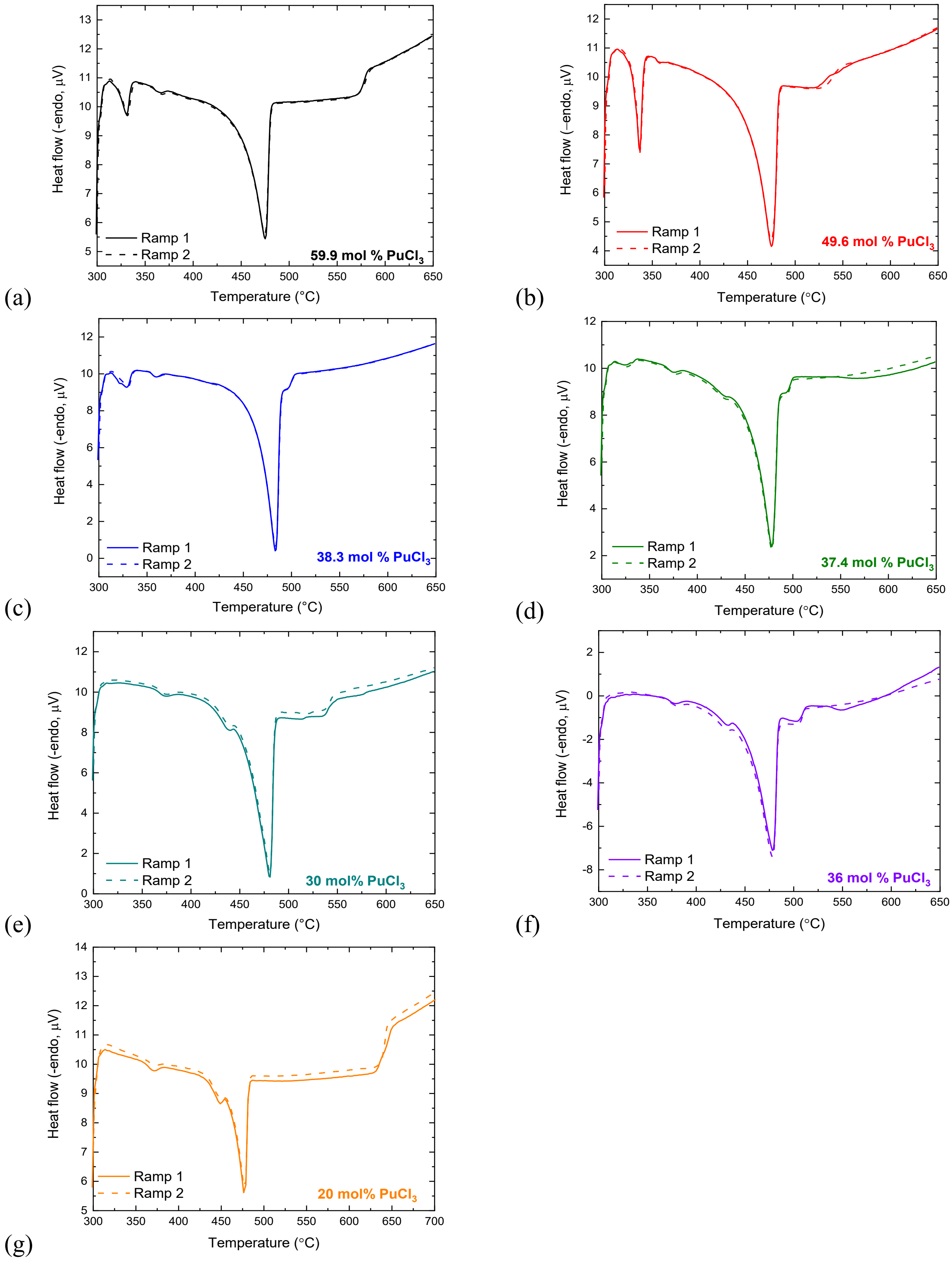

Figure 4. DSC responses of replicate analyses of (a) Salts 1, (b) Salt 2, (c) Salt 3, (d) Salt 4, (e) Salt 5, (f) Salt 6, and (g) Salt 7.

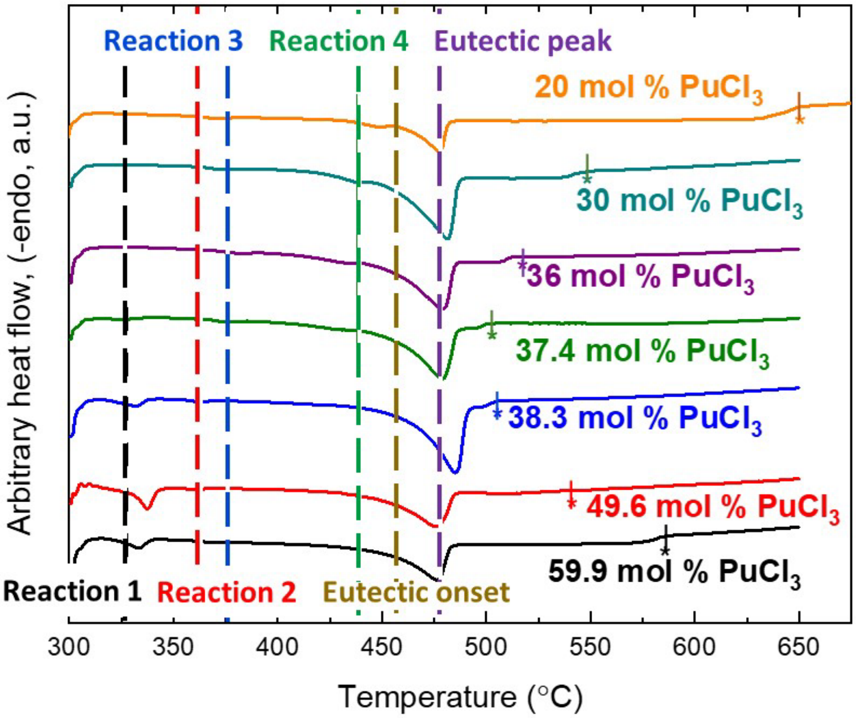

Figure 5. Representative DSC responses and average transition temperatures. Reaction 1 onset temperature (black dashed line), Reaction 2 peak temperature (red dashed line), Reaction 3 peak temperature (blue dashed line), Reaction 4 onset temperature (green dashed line), eutectic onset temperature (orange dashed line), eutectic peak temperature (purple dashed line) and liquidus temperatures are indicated by asterisks.

The eutectic reaction was observed for the seven mixtures at 457 ± 4 °C based on the onset temperatures. This is consistent with the NaCl-$PuCl_3$ eutectic melting at 453 ± 2 °C determined by Bjorklund et al. by using cooling curves. However, the transitions detected at temperatures below the eutectic onset temperature were not observed in previous measurements or predicted in any of the existing computationally assessed phase diagrams for the NaCl-$PuCl_3$ system (Yin et al., 2020; Beneš and Konings, 2008; Bjorklund et al., 1959). The occurrence of transitions below the eutectic temperature suggests that the NaCl-$PuCl_3$ mixtures may contain intermediate compounds. Intermediate compounds that undergo transition reactions at temperatures similar to transition temperatures detected in this work have been detected in other alkali chloride (KCl, RbCl, and CsCl)-$PuCl_3$ binary systems (Benz and Douglass, 1961, and Benz, Kahn and Leary, 1959). In particular, two intermediate compounds that undergo low temperature polymorphic transitions occur in the RbCl-$PuCl_3$ system: $RbPu_2Cl_7$ at 374 °C and Rb_3PuCl_6 at 398 °C (Benz and Douglass, 1961). Therefore, we speculate that the NaCl-$PuCl_3$ salts may contain analogous $NaPu_2Cl_7$, Na_2PuCl_5 and Na_3PuCl_6 compounds that behave similar to those formed in other binary alkali chloride-$PuCl_3$ systems. Structural characterization by X-ray diffraction will be performed in the future to confirm the presence of intermediate compounds.

Table 2. Measured Transition Temperatures of NaCl-$PuCl_3$ Salts

Salt ID	Mole % $PuCl_3$	Transition Temperatures (°C)						
		Reaction 1 Onset	Reaction 2 Peak	Reaction 3 Peak	Reaction 4 Onset	Eutectic Onset	Eutectic Peak	Liquidus Endpoint
Salt 1	59.9	322.7	368.2	ND*	ND	454.4	476.8	584.0
		322.5	367.0	ND	ND	454.8	477.6	581.7
Salt 2	49.6	330.1	359.2	ND	ND	453.2	475.0	530.5
		331.3	360.4	ND	ND	451.3	474.4	545.8
Salt 3	38.3	330.0	360.8	ND	ND	463.2	474.8	504.1
		328.9	359.8	ND	ND	464	475.2	501.2
Salt 4	37.4	326.0	ND	375.8	432.5	457.4	483.3	500.4
		324.3	ND	376.7	432.5	457.1	483.3	499.8
Salt 5	36.0	ND	ND	380.6	433.3	451.8	477.7	516.7
		ND	ND	380.2	433.2	452.6	478.0	512.0
Salt 6	30.0	ND	ND	375.5	440.8	544.4	478.2	546.2
		ND	ND	374.5	439.7	454.7	478.2	545.3
Salt 7	20.0	ND	ND	374.3	450.4	460.3	480.3	645.0
		ND	ND	371.8	449.1	461.8	480.6	650.0
Average		332	363	376	439	457	478	-
1 s		1	4	3	7	4	3	-

* ND = not detected.

4. Heat Capacity

4.1 Ratio Method

The Neztsch STA was used to measure heat capacity of Salt 4, which is the salt mixture nearest the eutectic composition. Several empty DSC crucibles and crucibles with known masses of a sapphire reference material were prepared following the procedure described in Section 3. The salt samples were thermally cycled within the STA over the temperature range of 20 to 650 °C prior to conducting the heat capacity measurements to melt the salt and establish good thermal contact with the crucible. The procedure for heat capacity measurements recommended in ASTM E1269 (ASTM 2018) was followed with modifications appropriate for analyzing molten salts. Three separate analyses were made under the same conditions to measure the instrumental background and response to heat flow. An analysis using two weight-matched empty crucibles was used to measure the instrument bias over the full temperature range and establish an instrumental baseline. Next, analysis of a sapphire standard and an empty crucible was used to measure the heat flow of a material with known heat capacity. Finally, analysis of a salt sample and empty crucible was used to measure the heat flow of the salt. The instrumental bias determined based on the heat flows measured during analysis of the two empty cells is automatically taken into account by the Netzsch PROTEUS® software during analyses of the sapphire and salts. The effect of temperature on sensitivity of the DSC response to heat flow was determined manually.

The three measurements used to determine the heat capacity of the salt in the liquid state were made using the same thermal profile: a 15-minute isothermal hold (producing no heat flow) at 520 °C, a linear ramp to 730 °C, and a 15-minute isothermal hold (producing no heat flow) at 730 °C. The three measurements used to determine the heat capacity of the salt in the solid state were made using the same thermal profile: a 15-minute isothermal hold (producing no heat flow) at 100 °C, a linear ramp to 300 °C, and a 15-minute isothermal hold (producing no heat flow) at 300 °C. The heat flows for the sapphire and salt sample measured at each temperature were automatically corrected for instrument bias by the Netzsch PROTEUS® software and further corrected for differences in heat flow measurement efficiencies at different temperatures manually. The heat capacity of the salt, C_p^s, is calculated based on the known heat capacity of sapphire by using the ratio of DSC responses during analyses of salt samples and sapphire as given in Equation 4.

$$C_\mathrm{p}^s = \frac{m_r}{m_s}\frac{\Delta\varphi_s}{\Delta\varphi_r} C_p^r + \frac{m_{cr}^r - m_{cr}^s}{m_s} C_p^{cr} \, , \tag{4}$$

where m_r and m_s are the masses of the sapphire reference material and the salt sample, m_{cr}^r and m_{cr}^s are the masses of the crucibles containing the sapphire and salt sample, $\Delta\varphi_r$ and $\Delta\varphi_s$ are the heat flows measured for the sapphire and salt sample corrected for the baseline and isothermal responses, and C_p^s, C_p^r and C_p^{cr} are the heat capacities of the salt sample, sapphire, and gold crucible, respectively. The heat capacity of sapphire provided by NIST (Ditmars, et al., 1982) and the heat capacity for gold provided in Arblaster (Arblaster, 2016) were used in the calculations. Weight matching of salt samples, sapphire, and crucibles was done to minimize the effect of dissimilar masses on the heat capacity values calculated using Equation 4. Gold crucibles used in DSC measurements were weight-matched to within 1.5% and the masses of the salt samples were matched to the mass of the sapphire reference material to within 1%. The mass of the sapphire was 22.06 mg and the gold crucible containing it was 384.84 mg.

4.2 Heat Capacity

The heat capacities of the two near-eutectic compositions Salt 4 (37.4 mol % $PuCl_3$) and Salt 3 (38.3 mol % $PuCl_3$) were measured between 100 and 300 °C to determine solid state heat capacity and between 520 and 730 °C to determine the liquid state heat capacity. The solid state heat capacities of Salt 1 (59.9 mol % $PuCl_3$) and Salt 7 (20 mol % $PuCl_3$) were also measured between 100 and 300 °C. The average and one standard deviation (error bars) of values from the three heat capacity analyses of each salt are shown in Figure 6. Salt 4 (37.4 mol % $PuCl_3$) and Salt 7

(20.0 mol % $PuCl_3$) samples had nearly identical solid heat capacity values of about 0.64 J g^{-1} K^{-1} at temperatures below 200 °C, the heat capacity values were significantly higher at temperatures above 200 °C. Similar behavior has been observed in the NaCl-KCl system (Sergeev, 2015**).** The heat capacities of Salts 1 and 3 are lower (about 0.55 J g^{-1} K^{-1}) from 100–200 °C. This is speculated to be an effect of intermediate compounds present in mixtures with higher $PuCl_3$ contents. The heat capacities of the liquid state of Salt 4 (37.4 mol % $PuCl_3$) and Salt 3 (38.3 mol % $PuCl_3$) show a slight positive correlation with temperature above 500 °C, on average increasing from 0.98 to 1.03 J g^{-1} K^{-1} for Salt 3 and from 1.08 to 1.14 J g^{-1} K^{-1} for Salt 4 over the range 600–725 °C. The differences in the heat capacity values of the liquid states parallel the differences in values for the solid states, with the $PuCl_3$-poor compositions having slightly higher heat capacity values than the $PuCl_3$-rich compositions. The averages and one standard deviation of the three heat capacity measurements for each sample measured at several temperatures are given in Table 3.

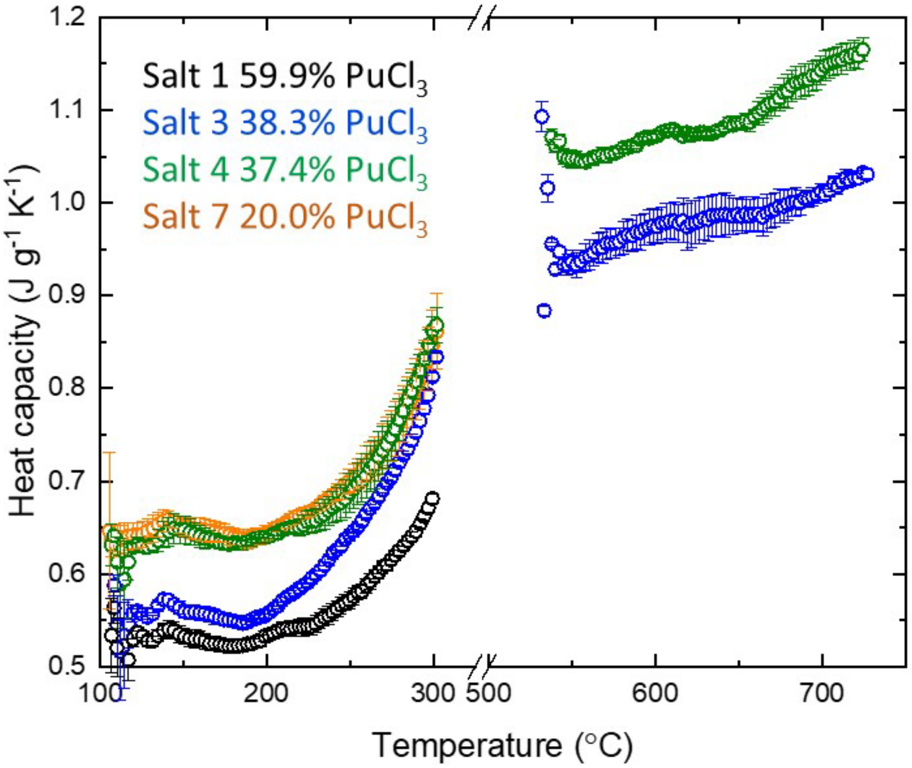

Figure 6. Averages of heat capacity values measured for Salt 1, Salt 3, Salt 4, and Salt 7. Error bars represent one standard deviation of three measurements.

Table 3. Heat Capacity Values for Four NaCl-$PuCl_3$ Salts, in J g^{-1} K^{-1}

Temperature (°C)	Salt 1	Salt 3	Salt 4	Salt 7
125	0.53±0.01	0.56±0.01	0.63±0.01	0.64±0.02
150	0.53±0.01	0.56±0.01	0.65±0.01	0.65±0.01
175	0.52±0.01	0.55±0.01	0.63±0.01	0.64±0.01
200	0.53±0.01	0.56±0.01	0.64±0.01	0.65±0.01
600	—	0.98±0.02	1.07±0.01	—
650	—	0.99±0.02	1.09±0.01	—
700	—	1.01±0.01	1.14±0.02	—
725	—	1.03±0.01	1.17±0.01	—

5. High Temperature DSC Crucibles

Use of DSC crucibles that are stable at high temperatures is necessary to measure the thermal and thermochemical behavior of molten fluoride salts over the range of temperatures that are of interest to MSR developers. Measurements at elevated temperature require a hermetic seal to maintain salt purity in the presence of atmospheric impurities and prevent loss of salt components (Piro, Lipkina, and Hallat, 2021). Analyses with salts sealed in the gold cells currently used at Argonne and elsewhere are limited to temperatures below approximately 800 °C because softening of gold and distortion of the cells occurs at higher temperatures. During FY 22, the use of several materials to fabricate DSC crucibles that could be mechanically sealed by the method and equipment used for commercial gold hermetically sealed crucibles was investigated. Three separate test series were conducted with cells fabricated of nickel and molybdenum, which were chosen for initial assessments due to their high corrosion resistance in salts and high melting temperatures. The first test series used hermetically sealed 5-mil thick stock Ni-201 crucibles, the second test series was with 20-mil thick pure molybdenum crucibles, and the third test series used 5-mil thick pure molybdenum crucibles. Results are summarized in the following sections.

5.1 Nickel Crucibles

Nickel is resistant to corrosive attack by the fluoride salts of interest to MSR developers (Piro, Lipkina, and Hallat, 2021 and McMurray et al., 2018). Nickel crucibles were fabricated at Argonne from sheet stock of Ni-201 metal to match the design of the commercially available gold cells. The final machined thickness was 5 mil. Figure 7a is a photograph of the hermetically sealed cell produced using the TA instruments press. The seal is buckled and folded irregularly compared to a satisfactory hermetic seal of a gold cell, which is shown in Figure 7b. The outer diameter of both cells is approximately 1 cm.

A 5-mil nickel crucible filled with a test salt was hermetically sealed and subjected to a heating cycle in the DSC to measure the integrity of the seal. The measured heat flow and mass are shown in Figure 8. The sudden decrease in the mass and decline in heat flow at temperatures above 850 °C are indications that the seal was not hermetic and salt was lost from the cell.

(a) (b)

Figure 7. Photographs of (a) sealed 5-mil nickel crucible and (b) sealed gold crucible.

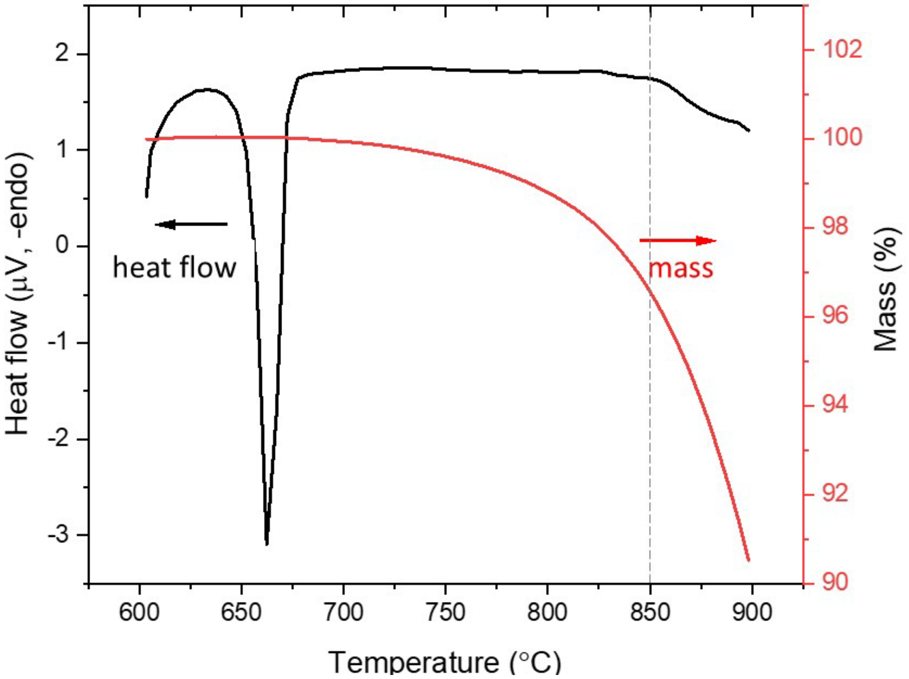

Figure 8. Heat flow and mass change of test salt in sealed 5-mil nickel crucible.

5.2 Molybdenum Crucibles

Molybdenum is a highly inert metal with a high melting point. Two sets of molybdenum crucibles were procured from outside vendors. The first set was obtained from Thermo Shield with a thickness of 20 mil. Attempts to hermetically seal these cells were not successful because the material was too thick for effective operation of the seal press. An incompletely sealed cell loaded with a test salt was heated in the DSC to confirm material compatibility. The heat flow and mass loss are plotted in Figure 9. Results indicate loss of salt from the cell at temperatures higher than 1000 °C, but negligible corrosion occurred.

A separate set of molybdenum crucibles was procured from Midwest Tungsten Service that had a final machined thickness of 5 mil. Crucibles fabricated from this material fractured during the initial pressing process. The photograph in Figure 10 is a bottom view of the crucible inverted on a piece of stock metal with the lip visible and surrounded by pieces of the lid that fractured during pressing. Other crucibles were annealed at 1000 °C for 1 h in an argon atmosphere prior to pressing to increase malleability. However, those crucibles were still too brittle and fractured during sealing.

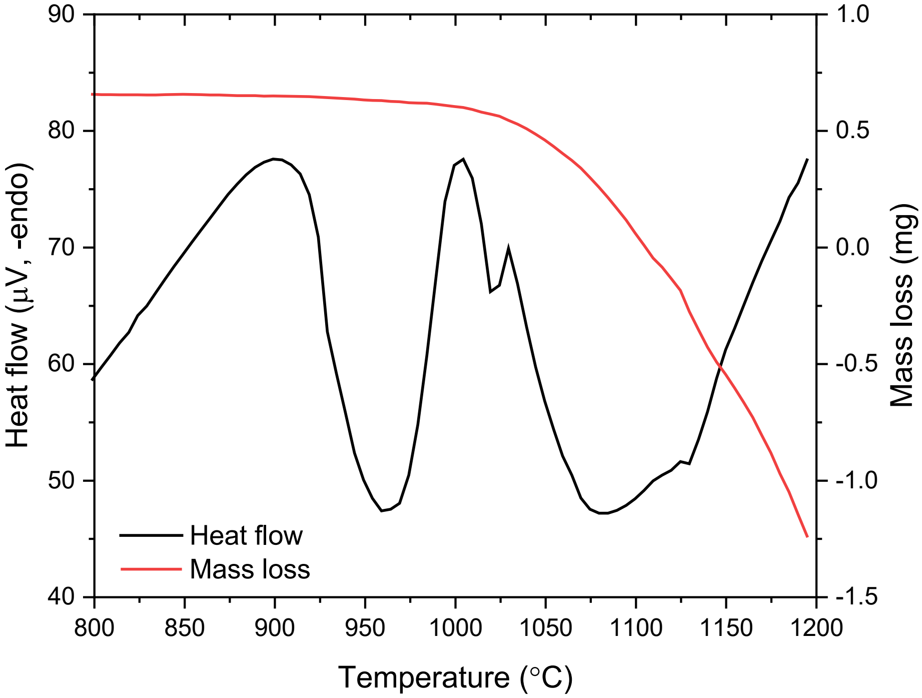

Figure 9. Heat flow and mass loss for an incompletely sealed molybdenum crucible fabricated by Thermo Shield.

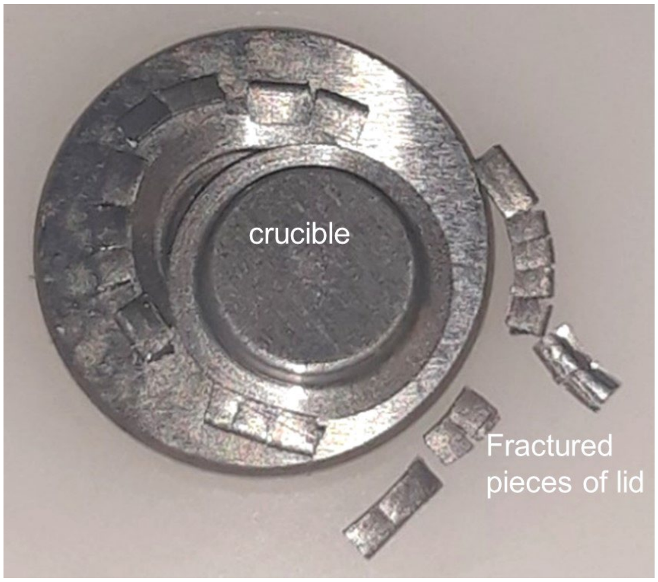

Figure 10. Photograph of 5-mil molybdenum crucible and lid that fractured during sealing.

6. Summary

Thermal properties of several compositions of the binary NaCl-$PuCl_3$ salt were measured to confirm the eutectic composition and provide high quality data for use by MSR developers. The $PuCl_3$ was generated by reducing PuO_2 to plutonium metal in the presence of calcium metal and then chlorinating the metallic plutonium with NH_4Cl. The resulting $PuCl_3$ was used to make seven binary NaCl-$PuCl_3$ compositions with between 59.9 mol % $PuCl_3$ (Salt 1) and 20.0 mol % $PuCl_3$ (Salt 7).

The eutectic temperature was measured to be 457 ± 4 °C by onset determination in DSC analyses of the seven mixtures, which is consistent with the values in the literature. Additional transitions were observed at approximately 332 and 363 °C in analyses of the Pu Cl_3-rich compositions (Salts 1-3) at about 376 and 439 °C in analyses the Na-rich compositions (Salts 4-7).

The solid state heat capacity decreased with increasing $PuCl_3$ content. The liquid state heat capacity was measured for Salt 3 (37.4 mol % $PuCl_3$) and Salt 4 (38.3 mol % $PuCl_3$). A higher heat capacity was measured for Salt 4 and measurements with both salts showed a positive correlation with temperature between 520 and 730 °C.

Cells fabricated from nickel and molybdenum for use in DSC measurements at high temperatures could not be adequately sealed because these materials are not sufficiently malleable, even after high-temperature annealing. It is recommended that future development focus on corrosion-resistant materials that have mechanical and thermal properties similar to the commercially available gold cells, such as Pt-Rh (80–20) and pure platinum. Those materials are chemically inert, soft, and malleable like gold, but have melting temperatures higher than 1000 °C (Rakhtsaum, 2013). Use of the Pt-Rh alloy should be evaluated first based on superior machinability for making precision parts and its current use in commercial DSC high temperature crucibles. The commercial Pt-Rh cells are not hermetically sealable, but it is expected that cells made from thinner stock can be sealed.

References

ASTM (2018). "Standard Test Method for Determining Specific Heat Capacity by Differential Scanning Calorimetry. E1269-11. ASTM-International, West Conschohcocken, PA https://doi.org/10.1520/E1269-11R18.

Arblaster, J.W. (2016). "Thermodynamic Properties of Gold." *J. Phase Equilibria Diffus. 37* 229–245. https://doi.org/10.1007/s11669-016-0449-z.

Ard, J.C., et al. (2022). "Development of the Molten Salt Thermal Properties Database − Thermochemical (MSTDB−TC), Example Applications, and LiCl−RbCl and UF_3−UF_4 System Assessments." *J. Nucl. Mater. 563*, 153631.

O. Beneš, R.J.M Konings. (2008). "Thermodynamic Evaluation of the NaCl-$MgCl_2$-UCl_3-$PuCl_3$ system." *J. Nucl. Mats. 375* 202–208.

Benz, R., R.M. Douglass. (1961). "Phase Equilibria in the Binary Systems $PuCl_3$-RbCl and $PuCl_3$-CsCl. *Journal of Physical Chemistry 65,* 1461–1463.

Benz, R., M. Kahn, J.A. Leary. (1959). "Phase Equilibria of the Binary System $PuCl_3$-KCl." *Journal of Physical Chemistry 63,* 1983–1984.

Bjorklund, C.W., J.G. Reavis, J.A. Learly, K.A. Walsh. (1959). "Phase Equilibria in the Binary Systems $PuCl_3$-NaCl and $PuCl_3$-LiCl." *Journal of Physical Chemistry 63*, 1774–1777.

D.A. Ditmars, S. Ishihara, S.S. Chang, G. Bernstein, E.D. West. (1982). "Enthalpy and Heat Capacity Standard Reference Material: Synthetic Sapphire (alpha -Al_2O_3) From 10 to 2250 K." *J. Res. Natl. Bur. Stand. (United States). 87*, 159–163. https://doi.org/10.6028/jres.087.012.

Höhne, G.W.H., W.F. Hemminger, H.-J. Flammersheim. (2003). Differential Scanning Calorimetry, 2nd ed., Springer,.

McMurray, J., T. Besmann, J. Jerden, M. Williamson, J. Ard, B. Fitzpatrick, M. Piro, A. Graham, Z. Taylor, B. Collins, B. Betzler, L. Qualls, T. Pandya, S. Greenwood, S. Johnson. (2018). *Multi-Physics Simulations for Molten Salt Reactor Evaluation: Chemistry Modeling and Database Development*. ORNL/SPR-2018/864

Piro, M.H.A., K. Lipkina, D. Hallat. (2021). "Exploring Crucible Designs for Differential Scanning Calorimetry Measurements of Fluoride Salts." *Thermochimica Acta. 699,* 178860.

G. Rakhtsaum. (2013). "Platnium Alloys: A Selective Review of the Available Literature." *Platinum Metals Review 57* 202–213.

Rose, M.A., S. Creasman. (2022). *Report on Data Quality Required for Modeling an MSR*. ANL/CFCT-22/17.

Sergeev, D., D. Kobertz, M. Müller. (2015). "Thermodynamics of the NaCl-KCl System." *Thermochimica Acta. 606*, 25-33.

Yin, H., J. Lin, B. Hu, W. Liu, X. Guo, Q. Liu, Z. Tang. (2020). “Thermodynamic Description of the Constitutive Binaries of the NaCl-KCl-UCl_3-$PuCl_3$ system.” Calphad. 70 101783.

Chemical and Fuel Cycle Technologies Division
Argonne National Laboratory
9700 South Cass Avenue, Bldg. 205
Lemont, IL 60439

www.anl.gov